Fungal Biology 129 (2025) 101526

Contents lists available at ScienceDirect

Fungal Biology

journal homepage: www.elsevier.com/locate/funbio

Role of putative APSES family transcription factor Swi6 in cell wall synthesis regulation in the agaricomycete *Pleurotus ostreatus*

Hayase Kojima [a,1], Takaya Izumi [a,1], Moriyuki Kawauchi [a,*], Yuitsu Otsuka [a], Kenya Tsuji [a], Akira Yoshimi [a,b], Chihiro Tanaka [a,b], Shigekazu Yano [c], Takehito Nakazawa [a], Yoichi Honda [a]

[a] Graduate School of Agriculture, Kyoto University, Kitashirakawaoiwakecho, Sakyo-ku, Kyoto, 606-8502, Japan
[b] Graduate School of Global Environmental Studies, Kyoto University, Kitashirakawaoiwakecho, Sakyo-ku, Kyoto, 606-8502, Japan
[c] Graduate School of Sciences and Engineering, Yamagata University, Jonan, Yonezawa, Yamagata, 992-8510, Japan

ARTICLE INFO

Handling Editor: Dr S Bates

Keywords:
APSES family transcription factor
Swi6
Cell wall integrity
Agaricomycete
Pleurotus ostreatus

ABSTRACT

Clade A APSES family transcription factor Swi6 functions alongside Mbp1 to form the MBF (MluI cell cycle box-binding factor) complex in ascomycetes. In the agaricomycete *Pleurotus ostreatus*, Mbp1 plays a crucial role in regulating β-glucan and chitin synthesis; however, the role of Swi6 has not been explored in this fungus. In this study, its involvement in cell wall synthesis regulation was analysed using *swi6* disruption strains in *P. ostreatus*. The Δ*swi6* strains exhibited reduced growth rates and shorter aerial hyphae formation in both agar and liquid media, suggesting an essential role of Swi6 in normal vegetative growth. Furthermore, *swi6* disruption affected cell wall thickness distribution, the expression of specific chitin synthase genes, the relative percentage of chitin, and sensitivity to calcofluor white, suggesting that Swi6 is required for normal chitin synthesis regulation in *P. ostreatus*. In contrast, no significant differences were observed between the wild-type and Δ*swi6* strains in the relative percentage of α- and β-glucan and the expression of α- and β-glucan synthase genes, suggesting its unimportant role in α- and β-glucan synthesis regulation. In conclusion, Swi6 is necessary for normal mycelial growth and chitin synthesis regulation in *P. ostreatus*. To the best of our knowledge, this study is the first report on the functional differences and overlaps between Mbp1 and Swi6 in the regulation of cell wall synthesis in agaricomycetes.

1. Introduction

The fungal cell wall, the outermost layer of the cell, is a crucial structure that provides mechanical strength, maintains cell shape, and protects against environmental stress. It comprises proteins and polysaccharides, including α-glucan, β-glucan, and chitin (Gow et al., 2017). In the pathogenic ascomycete *Aspergillus fumigatus*, widely used as a model organism of filamentous fungi, the inner rigid layer of the cell wall is rich in chitin, while the surface layer is primarily composed of α-glucan (Kang et al., 2018). However, in the agaricomycete *Schizophyllum commune*, although chitin is similarly abundant in the inner layer, β-glucan covers the surface layer (Ehren et al., 2020). These findings suggest that agaricomycetes possess a unique cell wall structure that differs significantly from that of ascomycetes. It is plausible that the regulatory mechanisms underlying this distinct cell wall structure also be fundamentally different. Agaricomycete cell walls are believed to be synthesised by various cell wall synthases, such as α-glucan synthase (Ags), β-glucan synthase (Fks), and chitin synthase (Chs) (Nakazawa et al., 2024). However, how these cell wall synthase genes are regulated remains unclear in agaricomycetes.

Our previous studies with *Pleurotus ostreatus* have highlighted the unique features of the basidiomycete cell wall. Using fluorescent probes that specifically bind to α- and β-glucan, DCD-tetraRFP and BGBD-GFP (Otsuka et al., 2022a, 2022b), hyphal surface of *P. ostreatus* is mainly covered by β-glucan, whereas that of the ascomycete *Aspergillus oryzae* is covered by α-glucan (Nakazawa et al., 2024). Furthermore, alkaline fractionation has revealed that *P. ostreatus* exhibited lower α-glucan content and higher β-glucan content in mycelial cell wall components

* Corresponding author.
E-mail address: kawauchi.moriyuki.8c@kyoto-u.ac.jp (M. Kawauchi).
[1] Equal Contribution.

https://doi.org/10.1016/j.funbio.2024.101526
Received 18 October 2024; Received in revised form 21 November 2024; Accepted 6 December 2024
Available online 9 December 2024

than *Aspergillus nidulans* (Miyazawa et al., 2018; Nakazawa et al., 2024). Additionally, four basidiomycete-specific chitin synthases (Chsb): Chsb1, Chsb2, Chsb3, and Chsb4 have been identified, of which Chsb2, Chsb3, and Chsb4 are required for normal cell wall structure formation *in P. ostreatus*. These chitin synthases are predicted to be responsible for forming a unique cell wall structure in basidiomycetes. As aforementioned, various aspects of the *P. ostreatus* cell wall have been extensively investigated, making it a suitable model organism for elucidating cell wall structure and synthesis regulation in agaricomycetes.

APSES family transcription factors, named after the first identified members Asm1, Phd1, Sok2, Efg1, and StuA, possess a highly conserved DNA-binding domain (the APSES domain) and play crucial roles in regulating various fungal developmental processes, including mating, cell cycle transition, cell wall synthesis, and pathogenicity. The APSES family transcription factors are divided into four clades: A, B, C, and D (Zhao et al., 2015). Clade A transcription factors: Mbp1, Swi4, and Swi6, can be further divided into two subclades, A-I and A-II, with Mbp1 and Swi4 belonging to A-I and Swi6 to A-II. In various ascomycetes, clade A members are reportedly involved in the regulation of cell wall synthesis (Chen et al., 2021; Dichtl et al., 2016; Huang et al., 2024; Qi et al., 2012). Additionally, in the agaricomycete *Ganoderma lucidum*, *Glswi6B*, one of two *swi6* gene splicing isoforms, is required for normal regulation of β-glucan and chitin synthesis (Lian et al., 2021). Clade A APSES family transcription factors share similar domain structures, making their identification challenging in various fungi. Therefore, our previous study has reorganised the evolutionary relationships among these transcription factors and revealed that Mbp1 and Swi6 are conserved across fungi, whereas Swi4 is specific to Saccharomycotina (Kojima et al., 2024). In *P. ostreatus*, two putative clade A APSES family transcription factors, protein ID 83192 and 134090 in the Joint Genome Institute database (https://mycocosm.jgi.doe.gov/PleosPC9_1/PleosPC9_1.home.html), have been identified as Mbp1 and Swi6, respectively (Kojima et al., 2024).

Investigation into the regulation of cell wall synthesis in *P. ostreatus* was first conducted using the disruption strains of *mbp1*. *mbp1* disruption decreases cell wall thickness, the relative percentage of β-glucan, and the expression of certain β-glucan and chitin synthase genes (Kojima et al., 2024). These results suggest that Mbp1 regulates β-glucan and chitin synthesis and thus contributes to the unique cell wall synthesis regulation specific to basidiomycetes in *P. ostreatus*. In the ascomycete yeast *Saccharomyces cerevisiae*, Mbp1 forms a heterodimer with Swi6, known as the MBF (MluI cell cycle box-binding factor) complex, and they function together (Koch et al., 1993). Similarly, in the filamentous ascomycetes *Beauveria bassiana* and *Fusarium verticillioides*, these two transcription factors can also form the MBF complex, suggesting partially overlapping functions (Ding et al., 2021; Huang et al., 2024; Koch et al., 1993). Therefore, it is possible that Swi6, in addition to Mbp1, is also a crucial element in regulating the cell wall synthesis in agaricomycetes. The division of roles between these two transcription factors needs further investigation to elucidate basidiomycete-specific regulatory mechanisms of cell wall synthesis. However, to the best of our knowledge, their functional redundancy and differences have not been investigated among agaricomycetes.

In this study, the function of Swi6 in regulating cell wall synthesis was analysed using *swi6* gene disruption strains and compared with that of Mbp1 in *P. ostreatus* to reveal the functional redundancy and differences between these two transcription factors.

2. Materials and methods

2.1. Strains, culture conditions, and genetic techniques

The *P. ostreatus* strains used in this study are listed in Table S1. For routine cultures, yeast extract, malt extract, and glucose (YMG) medium (Rao and Niederpruem, 1969) solidified with 2 % (w/v) agar in 90-mm Petri dishes, was used. Cultures were maintained at 28 °C in continuous darkness. The *swi6* gene disruption strains were obtained by gene targeting with homologous recombination, using the 20b strain as a host (Salame et al., 2012). For *P. ostreatus* transformation, the 20b strain was cultured in YMG liquid medium with shaking for 4 d, after which protoplasts were prepared from the mycelia using cellulase from *Aspergillus niger* (Sigma–Aldrich, St. Louis, MO, USA), Yatalase -Plus- (TaKaRa bio, Shiga, Japan), and β-glucanase from *Trichoderma longibrachiatum* (Sigma–Aldrich, St. Louis, MO, USA). DNA disruption cassettes were introduced into the protoplasts using the polyethylene glycol/calcium chloride method, as previously described (Nakazawa et al., 2016; Salame et al., 2012).

2.2. Construction of gene disruption cassettes

Three DNA fragments—the upstream and downstream regions of the *swi6* gene and the hygromycin B resistance gene (*hph*)—were fused using fusion PCR (Szewczyk et al., 2006). Genomic DNA of the *P. ostreatus* 20b strain was used as a template to amplify approximately 1.5 kb of the 5′ and 3′ flanking regions of *swi6*, and the pPHT1 plasmid to amplify the hygromycin resistance marker gene (*hph*) (Cummings et al., 1999). KOD FX Neo DNA polymerase (TOYOBO, Osaka, Japan) was used for the amplification and fusion of each fragment (Szewczyk et al., 2006). The fused fragment was purified using the Nucleospin PCR clean-up and gel extraction kit (TaKaRa bio, Shiga, Japan) and used as a disruption cassette. A schematic diagram of the *swi6* disruption cassette is depicted in Fig. S1A, and the primers used for PCR are listed in Table S2.

2.3. Genomic PCR

Crude genomic DNA extracted from the 20b strain and candidate transformants was used as templates (Izumitsu et al., 2012), and genomic PCR was performed using KOD FX Neo DNA polymerase (TOYOBO, Osaka, Japan). Integration of the *swi6* disruption cassette was confirmed through gene length change PCR (Fig. S1C), and the presence or absence of the *swi6* gene was verified using PCR amplification (Fig. S1D). Genomic PCR schematics are shown in Fig. S1B, gel electrophoresis results are presented Figs. S1C and S1D, and the primers used are listed in Table S2.

2.4. Growth and morphological observations

For observations of mycelial morphology and growth rate, 20 mL of autoclaved YMG agar medium was dispensed into Petri dishes (Φ90 mm) and a mycelium plug made with a cork borer (Φ8 mm) was inoculated into the centre of each plate. After 10 d of static cultivation in the dark at 28 °C, images of mycelia were captured using a scanner, and mycelial colony diameters were measured with a caliper.

For observations of aerial hyphae, 10 mL of YMG agar and liquid media were dispensed into test tubes (Φ16 mm) and autoclaved. A mycelium plug, made with a cork borer (Φ12 mm) was inoculated into the centre of each tube. After 10 d of static cultivation in the dark at 28 °C, images were captured to examine the height of aerial hyphae at the medium–gas interface.

For mycelial dry weight measurements, 40 mL of YMG liquid medium was dispensed into 100-mL flasks and autoclaved. A mycelium plug made with a cork borer (Φ8 mm) was inoculated into each flask. After 14 d of static cultivation in the dark at 28 °C, the mycelium was washed with water, hand-pressed with a paper towel, and freeze-dried. The dried mycelial weight was measured using an electronic balance.

2.5. Cell wall and hyphal observations

For cell wall observation, transmission electron microscopy (TEM) was performed. The 20b and *swi6* disruption strains were cultivated on Petri dishes (Φ90 mm) with 20 mL of YMG agar medium at 28 °C for 10 d. Observations were made after fixation and dehydration, as previously

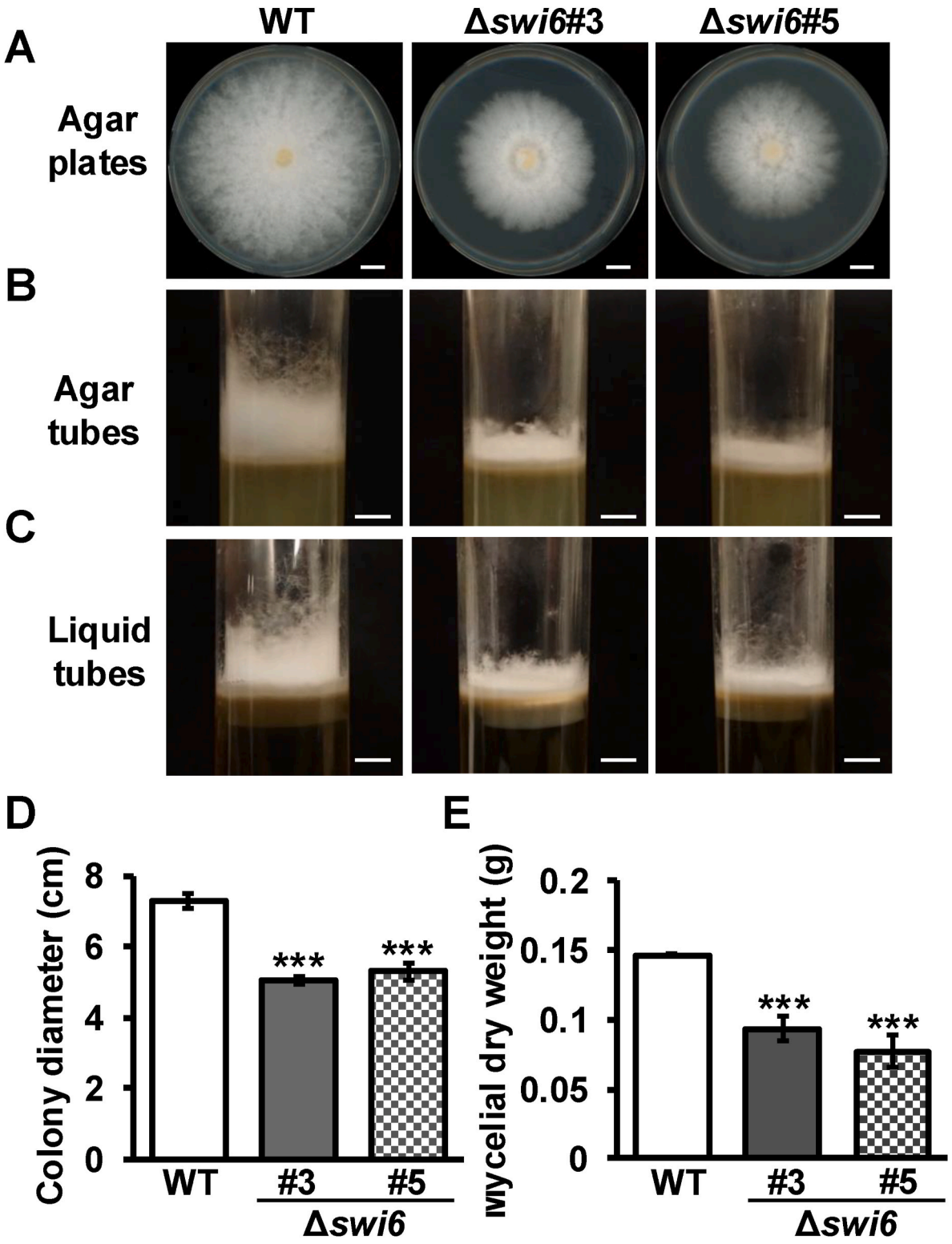

Fig. 1. Mycelial morphologies, aerial hyphae, and growth rates of the wild-type (WT) and Δ*swi6* strains. (A) Morphologies of mycelia grown on yeast extract, malt extract, and glucose (YMG) agar medium after 10 d (scale bar = 5 mm). Aerial hyphae of mycelia grown on YMG (B) agar and (C) liquid media after 10 d (scale bar = 5 mm). (D) Colony diameters of mycelia grown on YMG agar medium after 10 d. (E) Dry weight of mycelia grown on YMG liquid medium. Bars indicate standard deviations of three biological replicates ($n = 3$). Statistical significance was determined using a two-tailed equal variance *t*-test (***$P < 0.001$).

described (Han et al., 2023).

For hyphal observations, 40 mL of YMG medium was dispensed into 100-mL flasks and autoclaved. Ten mycelium plugs made with a cork borer (Φ8 mm) were inoculated into each flask and incubated at 28 °C for 5 d under shaking condition at 120 rpm. Hyphal surface chitin was then observed using 5 μL of 10 nmol/mL chitin-binding domain with an attached green fluorescent protein (ChBD-GFP) (Yano et al., 2011), as previously described (Kojima et al., 2024).

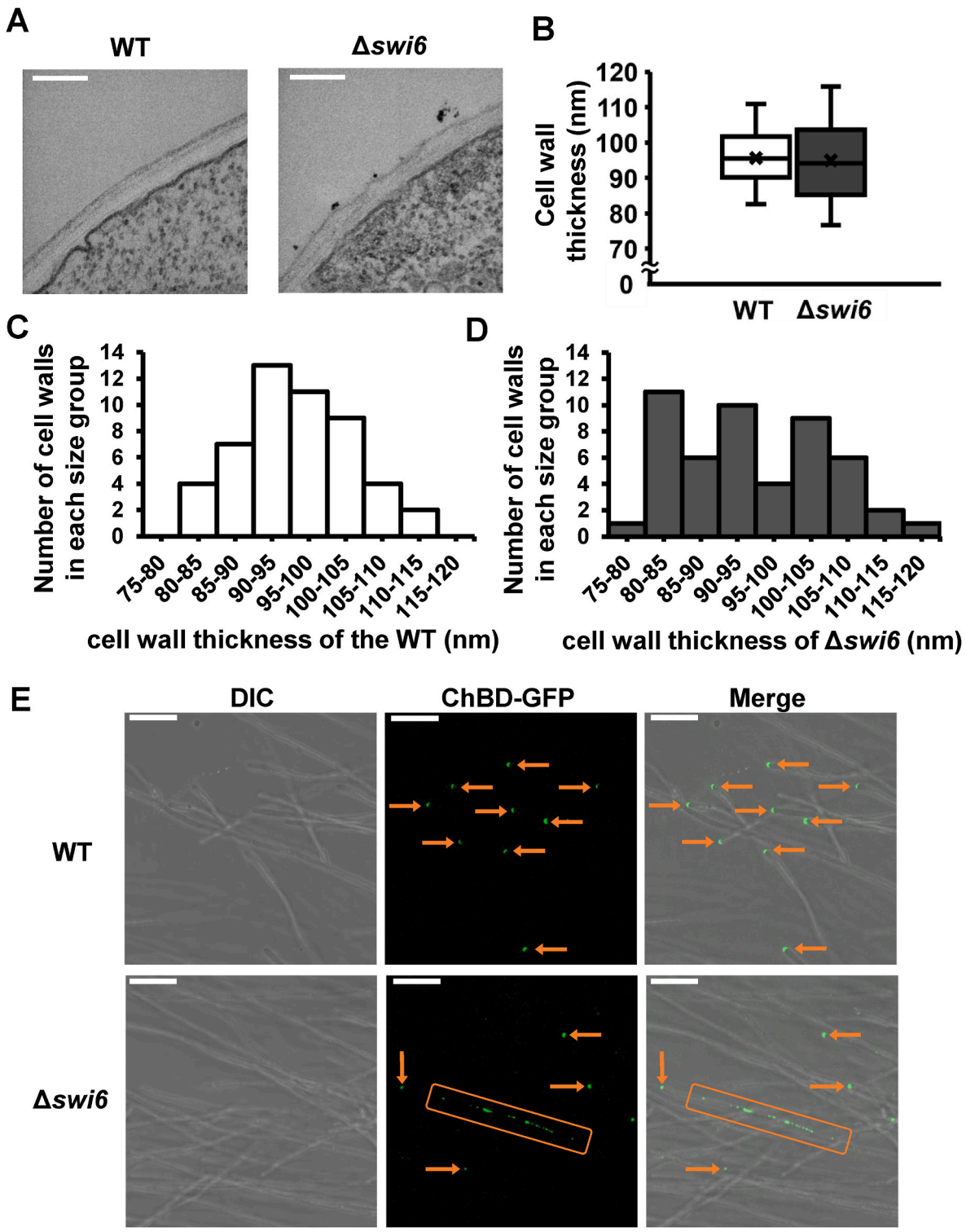

Fig. 2. Cell wall and hyphal morphologies of the wild-type (WT) and a Δ*swi6* strain. (A) Cell wall transmission electron microscopy (TEM) at ×40,000 magnification (scale bar = 200 nm). (B) Measurements of cell wall thickness under TEM observations; the bars indicate the standard deviations (n = 50). Cell wall thickness distributions in (C) the WT and (D) Δ*swi6*. (E) Chitin staining using the chitin-specific fluorescent probe (ChBD-GFP) under a confocal microscope (scale bar = 20 μm); orange arrows indicate ChBD-GFP fluorescence at hyphal tips in the WT and Δ*swi6*; orange round rectangles indicate increased fluorescence in Δ*swi6*. DIC: images obtained by optical microscopy with differential interference contrast. Merge: images merged DIC and ChBD-GFP fluorescence images.

2.6. Quantitative reverse-transcription PCR (qRT-PCR)

Autoclaved YMG agar (20 mL) was dispensed into Petri dishes (Φ90 mm). After solidifying, a single layer of autoclaved cellophane was added to cover the entire plate. A mycelium plug made with a cork borer (Φ8 mm) was inoculated into the centre of each plate and incubated for 14 d in the dark at 28 °C. After incubation, mycelia were peeled from the cellophane and used for RNA extractions, followed by qRT-PCR as previously described (Kojima et al., 2024). The primer sets used for the amplification of cDNA fragments and their amplification efficiencies are

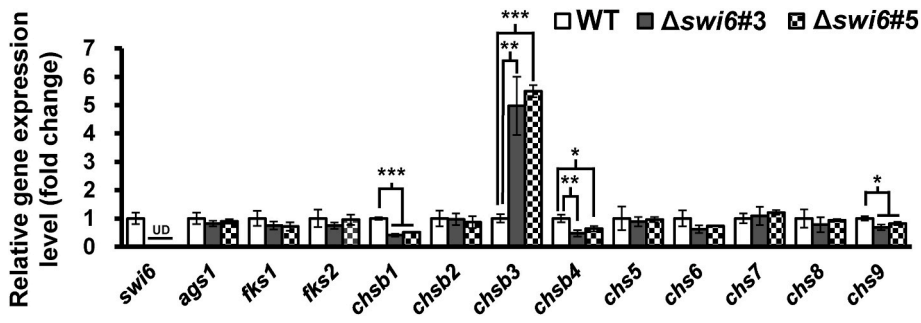

Fig. 3. Relative gene expression levels of cell wall synthase genes (*ags*: α-glucan synthase, *fks*: β-glucan synthase, *chs*: chitin synthase) in the wild-type (WT) and Δ*swi6* strains. The bars indicate standard deviations of three biological replicates ($n = 3$). Statistical significance was determined using a two-tailed equal variance *t*-test (*$P < 0.05$, **$P < 0.01$, ***$P < 0.001$). UD: undetermined.

listed in Table S3.

2.7. Glucan and chitin measurements

For glucan and chitin measurements, 20 mL of autoclaved YMG agar was dispensed into Petri dishes (Φ90 mm). After solidifying, a single layer of autoclaved cellophane was added to cover the entire plate. A mycelium plug made with a cork borer (Φ8 mm) was then inoculated into the centre of each plate and incubated for 14 d in the dark at 28 °C. After incubation, mycelia were peeled from the cellophane using a sterile spatula, ground into powder using liquid nitrogen and a mortar and pestle, and freeze-dried. For glucan and chitin measurements, a β-Glucan Assay Kit (Yeast and Mushroom) (Megazyme, Bray, Ireland) and a D-Glucosamine Assay Kit (Megazyme, Bray, Ireland) were used, respectively, as previously described (Schiphof et al., 2024).

Total glucan measurements were conducted using freeze-dried mycelia hydrolysed with sulfuric acid (H_2SO_4) and reagents in the assay kit, and α-glucan, along with a small amount of background glucose, was measured using the freeze-dried mycelia treated with 1.7 N NaOH and the amyloglucosidase, invertase, and trehalase in the assay kit. Chitin measurement was conducted using the freeze-dried mycelia hydrolysed with 4 N HCl.

2.8. Stress resistance assay

Autoclaved YMG agar medium was supplemented with 0.02 % sodium dodecyl sulfate (SDS) and 5 mM H_2O_2 to test the resistance to the cell membrane and oxidative stressors. Additionally, 500 μg/mL calcofluor white (CFW) and 100 μg/mL micafungin (MF) were used to test resistance to cell wall synthesis inhibitors. Fluorescent Brightener 28 disodium salt solution (Sigma–Aldrich) and Funguard (Astellas, Tokyo, Japan) were used for CFW and MF assays, respectively. YMG agar without stressors was used as a control. A mycelium plug made with a cork borer (Φ8 mm) was inoculated into the centre of each plate. After 10 d of cultivation in the dark at 28 °C, images were captured using a scanner, and the relative inhibitory rates were calculated as previously described (Kojima et al., 2024).

3. Results

3.1. Disruption of swi6 affects mycelial morphology

Functional differences and overlaps between Mbp1 and Swi6 have not been well understood among filamentous fungi. To investigate this, the Swi6 function was analysed using *swi6* disruption strains. Since the splicing isoforms of *swi6* have been reported in the agaricomycete *G. lucidum* (Lian et al., 2021), alternative splicing was examined based on the predicted intron positions in the *P. ostreatus swi6* gene locus. In this study, no *swi6* splicing isoforms were observed at the predicted intron locations, as only one band appeared in PCR amplifications (Fig. S2). Therefore, the *swi6* gene disruption cassette was designed to knock out the entire region of the predicted *swi6* gene in *P. ostreatus* and used for transformation (Figs. S1A and B). As a result of the transformation, five transformants were obtained and integration of the *swi6* disruption cassette and the absence of the *swi6* gene were confirmed in these strains through genomic PCR (Figs. S1C and D). Among these strains, Δ*swi6*#3 and Δ*swi6*#5 were randomly selected. These two independent strains were used along with the parental strain 20b as the wild-type strain (WT) for subsequent experiments.

On YMG agar medium, the mycelial colony size of Δ*swi6* strains was reduced by approximately 30 % compared to that of the WT (Figs. 1A and D). Similarly, on YMG liquid medium, the mycelial dry weight of Δ*swi6* strains was approximately 30 % lower than that of the WT (Fig. 1E). These results indicate Δ*swi6* strains exhibited reduced growth rates on both agar and liquid media. Additionally, Δ*swi6* strains developed shorter aerial hyphae than the WT in both conditions (Figs. 1B and C). Therefore, Swi6 is essential for normal aerial hyphae formation in both solid and liquid conditions.

3.2. swi6 is required for normal cell wall synthesis regulation

To investigate the effect of *swi6* disruption on cell wall formation, cell walls and hyphal surface chitin were observed in the WT and Δ*swi6* strains (Fig. 2). TEM observations revealed no significant differences in the average cell wall thickness between the WT and Δ*swi6* (Figs. 2A and B). However, the dispersion of cell wall thickness increased in Δ*swi6* (Fig. 2B). Additionally, the WT and Δ*swi6* differed in cell wall thickness distribution, with a unimodal distribution observed in the WT (Fig. 2C) and a multimodal distribution in Δ*swi6* (Fig. 2D). A chitin-specific fluorescent probe, ChBD-GFP (Yano et al., 2011), was used to observe chitin on the hyphal surface (Fig. 2E). In the WT, ChBD-GFP fluorescence was observed exclusively at the hyphal tips, whereas in Δ*swi6*, fluorescence was detected not only at the tips but also sparsely throughout the hyphal area. These results suggest that disruption of *swi6* causes abnormal regulation of cell wall synthesis.

3.3. Swi6 plays a crucial role in chitin synthesis regulation

First, the expression of *swi6* was examined using qRT-PCR to confirm its transcriptional inactivation. As a result, no expression of *swi6* was detected (Fig. 3). Then, the relative expression levels of cell wall synthase genes were examined (Fig. 3) to clarify the role of Swi6 in regulating cell wall synthase genes. No significant differences were observed between the WT and Δ*swi6* strains in the relative expression levels of the α-glucan synthase gene, *ags1*, and the β-glucan synthase genes, *fks1* and *fks2*. In contrast, the relative expression levels of three chitin synthase genes, *chsb1*, *chsb4*, and chs9 were significantly decreased by approximately 55 %, 45 %, and 25 %, respectively, whereas the level of *chsb3* increased approximately five-fold in Δ*swi6* strains. Additionally, the relative percentages of major cell wall polysaccharides—α-glucan,

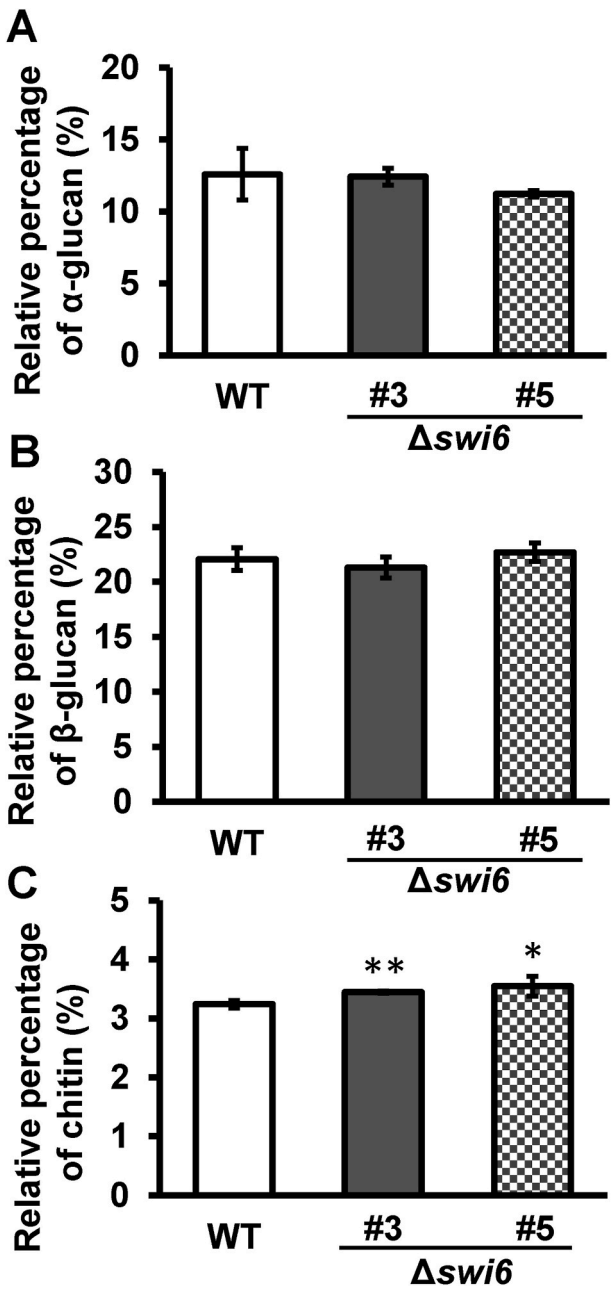

Fig. 4. Relative percentages of (A) α-glucan, (B) β-glucan, and (C) chitin in mycelial dry weight. The bars indicate standard deviations of three biological replicates ($n = 3$). Statistical significance was determined using a two-tailed equal variance *t*-test (*$P < 0.05$, **$P < 0.01$).

β-glucan, and chitin (g/100-g dried mycelium)—were measured. The relative percentages of α- and β-glucan remained unchanged between the WT and Δ*swi6* strains (Figs. 4A and B), whereas chitin levels were slightly elevated in Δ*swi6* strains (Fig. 4C). These findings suggest that Swi6 plays a crucial role in regulating normal chitin synthesis.

3.4. swi6 disruption alters sensitivity to chitin synthesis inhibitor and oxidative stress

To investigate the role of Swi6 in mediating responses to cell wall and environmental stresses in *P. ostreatus*, stress resistance assays were performed (Fig. 5A). First, the sensitivities of the WT and Δ*swi6* strains to cell wall synthesis inhibitors were examined. Compared to the WT, Δ*swi6* strains exhibited increased sensitivity to CFW, a chitin synthesis inhibitor, while their resistance to MF, a β-glucan synthesis inhibitor, remained unchanged (Fig. 5B). Additionally, studies in *G. lucidum* have revealed that *Glswi6* silencing enhances the growth inhibitory effects of SDS and H_2O_2 (Lian et al., 2021; Zhang et al., 2018), and thus, these compounds were used to assess whether Swi6 of *P. ostreatus* contributes to resistance against cell membrane and oxidative stress. In *P. ostreatus*, no significant differences in SDS resistance were observed between the WT and Δ*swi6* strains (Fig. 5C). However, Δ*swi6* strains exhibited greater sensitivity to H_2O_2 than other stressors (Fig. 5C). Therefore, Swi6 plays a key role in regulating cell wall synthesis in response to chitin synthesis inhibition and oxidative stress.

4. Discussion

In this study, the role of putative APSES family transcription factor Swi6 in regulating cell wall synthesis was investigated using Δ*swi6* strains in the agaricomycete *P. ostreatus*. In the Δ*swi6* strains, the relative percentages of α- and β-glucan and the relative gene expression levels of their respective synthases remained unchanged compared to the WT (Figs. 3, 4A and B). Therefore, Swi6 does not appear to regulate α- and β-glucan synthesis. On the other hand, the slight increase in the relative percentage of chitin was observed despite the reduced gene expression of *chsb1*, *chsb4*, and *chs9* (Figs. 3 and 4C). This may be caused by the increased gene expression of *chsb3*. These results suggest abnormal chitin synthesis regulation in Δ*swi6* strains. TEM observations revealed an abnormal distribution of cell wall thickness in Δ*swi6* strains (Figs. 2C and D) despite no difference in the average thickness (Figs. 2A and B). This suggests that polysaccharide synthesis occurs unevenly along the hyphae, with certain areas producing either more or less polysaccharide than the WT. Given that chitin serves as a fundamental structure supporting glucans and other polysaccharides (Ehren et al., 2020; Gow et al., 2017), this uneven cell wall synthesis is likely influenced by possible structural changes in chitin, such as differences in distribution, molecular weight and interactions with other polysaccharides, caused by abnormal chitin synthesis regulation in Δ*swi6* strains. Furthermore, Δ*swi6* strains exhibited increased ChBD-GFP fluorescence compared to the WT (Fig. 2E). Since chitin is connected to β-glucan in the cell wall (Gow et al., 2017), the observed abnormalities in chitin may have weakened its interaction with the β-glucan, which covers cell wall surface, leading to increased chitin exposure at the cell wall surface. Additionally, the increased sensitivity of Δ*swi6* strains to CFW, a chitin synthesis inhibitor (Fig. 5B), further supports that chitin synthesis is not normally regulated. These findings suggest that Swi6 plays a crucial role in the normal regulation of chitin synthesis.

In ascomycetes, Swi6 forms a heterodimer with Mbp1, known as the MBF complex, and functions together with it (Ding et al., 2021; Huang et al., 2024; Koch et al., 1993). However, whether Swi6 and Mbp1 work together in agaricomycetes remains unclear. If they do, Mbp1 and Swi6 are likely to share common functions. In *P. ostreatus*, both Δ*mbp1* and Δ*swi6* strains exhibited increased sensitivity to CFW, an approximately 5-fold increase in the relative expression level of *chsb3*, and reduced expression of *chsb1*, *chsb4*, and *chs9* (Figs. 3 and 5B) (Kojima et al., 2024). However, unlike *swi6* disruption, *mbp1* disruption results in thinner cell walls, decreased expression of *fks1* and *fks2*, and reduced β-glucan content (Figs. 2A, B, 3 and 4B) (Kojima et al., 2024). Additionally, the cell wall thickness of Δ*mbp1* exhibited a unimodal distribution, similar to that of the WT (Figs. 2C and S3), while that of Δ*swi6* exhibited a multimodal distribution (Fig. 2D). Overall, Swi6 may regulate chitin synthesis together with Mbp1, whereas Mbp1 might regulate β-glucan synthesis independently. In addition to their role in cell wall synthesis regulation, both *mbp1* and *swi6* disruptions cause reduced growth rate and shorter aerial hyphae in both agar and liquid media (Fig. 1) (Kojima et al., 2024), indicating their importance for normal mycelial growth under these conditions. Moreover, increased sensitivity to H_2O_2 was observed in both Δ*mbp1* and Δ*swi6* strains (Fig. 5C) (Kojima et al., 2024), suggesting their crucial role in the response to oxidative

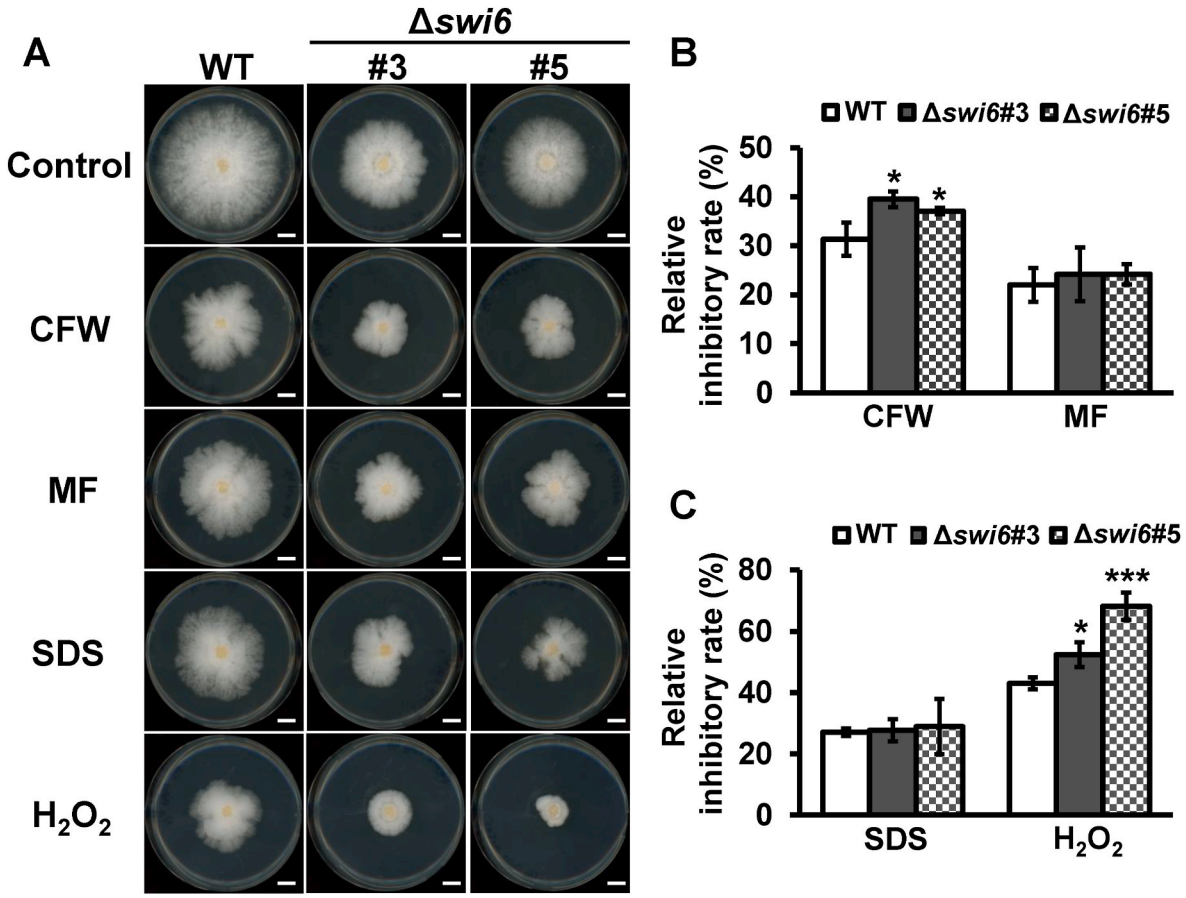

Fig. 5. Stress resistance to the cell wall and environmental stress in the wild-type (WT) and Δ*swi6* strains. (A) Mycelial morphology grown on yeast extract, malt extract, and glucose (YMG) agar media supplemented with 500 μg/mL calcofluor white (CFW), 100 μg/mL micafungin (MF), 0.02% sodium dodecyl sulfate (SDS), and 5 mM H_2O_2 after 10 d (scale bar = 5 mm). The relative growth inhibitory rates of the WT and Δ*swi6* mycelia grown on YMG media supplemented with (B) cell wall synthesis inhibitors (CFW and MF) and (C) cell membrane and oxidative stressors (SDS and H_2O_2) are shown. The bars indicate standard deviations of three biological replicates ($n = 3$). Statistical significance was determined using a two-tailed equal variance *t*-test (*$P < 0.05$, ***$P < 0.001$).

stress. Overall, Swi6 and Mbp1 may have partially overlapping functions in *P. ostreatus*.

Compared to previous studies with the agaricomycete *G. lucidum*, similar results were obtained in the stress resistance tests for CFW and H_2O_2. Both *swi6* disruption in *P. ostreatus* and *Glswi6* silencing in *G. lucidum* increased the sensitivity to these compounds (Figs. 5B and C) (Lian et al., 2021; Zhang et al., 2018). However, our present study highlighted the crucial differences in Swi6 function between *P. ostreatus* and *G. lucidum*. In *G. lucidum*, *Glswi6* silencing leads to reduced resistance to SDS, decreased cell wall thickness, lower β-glucan and chitin content, and reduced expression of certain putative glucan synthase genes (Lian et al., 2021). Additionally, overexpression of *Glswi6B*, one of the *Glswi6* splicing isoforms, conversely increases β-glucan and chitin synthesis (Lian et al., 2021). Therefore, *Glswi6B* is believed to regulate both β-glucan synthesis and chitin synthesis in *G. lucidum* (Lian et al., 2021), but these results differ from ours (Figs. 2A, B, 3, 4B, C, and 5C). Given that *P. ostreatus* belongs to the Agaricales and *G. lucidum* to the Polyporales, Swi6 appears to be functionally differentiated between these orders. Furthermore, in *P. ostreatus*, no *swi6* splicing isoforms were observed at the predicted intron locations in this study (Fig. S2). Conversely, *G. lucidum* possess the two splicing isoforms, *Glswi6A* and *Glswi6B* (Lian et al., 2021). This highlights significant differences in both the regulation of *swi6* expression and its function between these two fungal species. However, these differences may be attributed to methodological differences: our study used gene knockout in *P. ostreatus*, whereas *G. lucidum* studies used gene silencing and overexpression (Lian et al., 2021; Zhang et al., 2018). In *G. lucidum*, *Glswi6*-silenced strains exhibit visible defects in fruiting body formation (Zhang et al., 2018). To compare the functions of *swi6* between the Agaricales and the Polyporales, the effects of *swi6* disruption on fruiting body formation will be investigated in *P. ostreatus*.

5. Conclusion

P. ostreatus possesses two putative clade A APSES family transcription factors, Mbp1 and Swi6. Disruption of *swi6* affected cell wall thickness distribution, the expression of specific chitin synthase genes, the relative percentage of chitin, and CFW sensitivity, indicating that Swi6 plays a crucial role in normal chitin synthesis regulation in *P. ostreatus*. Based on the results of qRT-PCR analysis, it is plausible that Swi6 may regulate chitin synthesis alongside Mbp1. In contrast, Swi6 may not be essential for glucan synthesis regulation. Mbp1 is necessary for normal β-glucan synthesis regulation, indicating that it regulates β-glucan synthesis independently of Swi6 in *P. ostreatus*. This study is the first to reveal functional differences and overlaps between Mbp1 and Swi6 in regulating cell wall synthesis in agaricomycetes, marking a crucial step toward elucidating the evolutionary functional divergence of Mbp1 and Swi6.

CRediT authorship contribution statement

Hayase Kojima: Writing – original draft, Visualization, Methodology, Investigation, Formal analysis, Data curation, Conceptualization. **Takaya Izumi:** Writing – review & editing, Visualization, Methodology,

Investigation, Formal analysis, Data curation, Conceptualization. **Moriyuki Kawauchi:** Writing – review & editing, Visualization, Supervision, Resources, Methodology, Funding acquisition, Formal analysis, Conceptualization. **Yuitsu Otsuka:** Methodology, Investigation, Data curation. **Kenya Tsuji:** Resources, Funding acquisition, Data curation. **Akira Yoshimi:** Resources, Funding acquisition, Data curation. **Chihiro Tanaka:** Resources, Project administration, Data curation. **Shigekazu Yano:** Resources, Methodology. **Takehito Nakazawa:** Methodology, Data curation. **Yoichi Honda:** Writing – review & editing, Resources, Project administration, Data curation, Conceptualization.

Data availability

Data will be made available on request.

Funding sources

This work was supported in part by the Institute for Fermentation, Osaka, Japan (K-2019-002 to M. K. and K. T.), the Grants-in-Aid for Scientific Research from the Japan Society for the Promotion of Science (22H02238 to A. Y. and M. K., 22K05763, 24KK0119 to M. K.), the Grant-in-Aid for JSPS Fellows (23KJ1191 to Y. O.), and the JSPS Bilateral Program (JPJSBP 120238807 to M. K.).

Declaration of competing interest

The authors declare that they have no known competing financial interests or personal relationships that could have appeared to influence the work reported in this paper.

Acknowledgments

The authors thank Prof. Yitzhak Hadar (Hebrew University of Jerusalem) for providing *P. ostreatus* strain 20b. We thank the Division of Electron Microscopic Study, Centre for Anatomical Studies, Graduate School of Medicine, Kyoto University, for technical assistance with electron microscopy.

Appendix A. Supplementary data

Supplementary data to this article can be found online at https://doi.org/10.1016/j.funbio.2024.101526.

References

Chen, X., Lu, Z., Chen, Y., Wu, R., Luo, Z., Lu, Q., Guan, N., Chen, D., 2021. Deletion of the *MBP1* gene, involved in the cell cycle, affects respiration and pseudohyphal differentiation in *Saccharomyces cerevisiae*. Microbiol. Spectr. 9, e0008821.

Cummings, W.J., Celerin, M., Crodian, J., Brunick, L.K., Zolan, M.E., 1999. Insertional mutagenesis in *Coprinus cinereus*: use of a dominant selectable marker to generate tagged, sporulation-defective mutants. Curr. Genet. 36, 371–382.

Dichtl, K., Samantaray, S., Wagener, J., 2016. Cell wall integrity signalling in human pathogenic fungi. Cell Microbiol. 18, 1228–1238.

Ding, J.L., Hou, J., Li, X.H., Feng, M.G., Ying, S.H., 2021. Transcription activator Swi6 interacts with Mbp 1 in MluI cell cycle box-binding complex and regulates hyphal differentiation and virulence in *Beauveria bassiana*. J. Fungi 7, 411.

Ehren, H.L., Appels, F.V.W., Houben, K., Renault, M.A.M., Wösten, H.A.B., Baldus, M., 2020. Characterization of the cell wall of a mushroom forming fungus at atomic resolution using solid-state NMR spectroscopy. Cell Surf 6, 100046.

Gow, N.A.R., Latge, J.P., Munro, C.A., 2017. The fungal cell wall: structure, biosynthesis, and function. Microbiol. Spectr. 5. https://doi.org/10.1128/microbiolspec.FUNK-0035-2016.

Han, J., Kawauchi, M., Schiphof, K., Terauchi, Y., Yoshimi, A., Tanaka, C., Nakazawa, T., Honda, Y., 2023. Features of disruption mutants of genes encoding for hydrophobin Vmh2 and Vmh3 in mycelial formation and resistance to environmental stress in *Pleurotus ostreatus*. FEMS Microbiol. Lett. 370, fnad036.

Huang, Y., Chen, J., Xia, H., Gao, Z., Gu, Q., Liu, W., Tang, G., 2024. FvMbp1-Swi6 complex regulates vegetative growth, stress tolerance, and virulence in *Fusarium verticillioides*. J. Hazard Mater. 473, 134576.

Izumitsu, K., Hatoh, K., Sumita, T., Kitade, Y., Morita, A., Tanaka, C., Gafur, A., Ohta, A., Kawai, M., Yamanaka, T., Neda, H., Ota, Y., 2012. Rapid and simple preparation of mushroom DNA directly from colonies and fruiting bodies for PCR. Mycoscience 53, 396–401.

Kang, X., Kirui, A., Muszyński, A., Widanage, M.C.D., Chen, A., Azadi, P., Wang, P., Mentink-Vigier, F., Wang, T., 2018. Molecular architecture of fungal cell walls revealed by solid-state NMR. Nat. Commun. 9, 2747.

Koch, C., Moll, T., Neuberg, M., Ahorn, H., Nasmyth, K., 1993. A role for the transcription factors Mbp1 and Swi4 in progression from G1 to S phase. Science 261, 1551–1557.

Kojima, H., Kawauchi, M., Otsuka, Y., Schiphof, K., Tsuji, K., Yoshimi, A., Tanaka, C., Yano, S., Nakazawa, T., Honda, Y., 2024. Putative APSES family transcription factor *mbp1* plays an essential role in regulating cell wall synthesis in the agaricomycete *Pleurotus ostreatus*. Fungal Genet. Biol. 175, 103936.

Lian, L., Zhang, G., Zhu, J., Wang, Y., Wang, L., Liu, R., Shi, L., Ren, A., Zhao, M., 2021. Swi6B, an alternative splicing isoform of Swi6, mediates the cell wall integrity of *Ganoderma lucidum*. Environ. Microbiol. 23, 4405–4417.

Miyazawa, K., Yoshimi, A., Kasahara, S., Sugahara, A., Koizumi, A., Yano, S., Kimura, S., Iwata, T., Sano, M., Abe, K., 2018. Molecular mass and localization of α-1,3-glucan in cell wall control the degree of hyphal aggregation in liquid culture of *Aspergillus nidulans*. Front. Microbiol. 9, 2623.

Nakazawa, T., Kawauchi, M., Otsuka, Y., Han, J., Koshi, D., Schiphof, K., Ramírez, L., Pisabarro, A.G., Honda, Y., 2024. *Pleurotus ostreatus* as a model mushroom in genetics, cell biology, and material sciences. Appl. Microbiol. Biotechnol. 108, 217.

Nakazawa, T., Tsuzuki, M., Irie, T., Sakamoto, M., Honda, Y., 2016. Marker recycling via 5-fluoroorotic acid and 5-fluorocytosine counter-selection in the white-rot agaricomycete *Pleurotus ostreatus*. Fungal Biol. 120, 1146–1155.

Otsuka, Y., Sasaki, K., Suyotha, W., Furusawa, H., Miyazawa, K., Konno, H., Yano, S., 2022a. Construction of a fusion protein consisting of α-1,3-glucan-binding domains and tetrameric red fluorescent protein, which is involved in the aggregation of α-1,3-glucan and inhibition of fungal biofilm formation. J. Biosci. Bioeng. 133, 524–532.

Otsuka, Y., Sato, K., Yano, S., Kanno, H., Suyotha, W., Konno, H., Makabe, K., Taira, T., 2022b. GH-16 type β-1,3-glucanase from lysobacter sp. MK9-1 enhances antifungal activity of GH-19 type chitinase, and its glucan-binding domain binds to fungal cell-wall. J. Appl. Glycosci. 69, 49–56.

Qi, Z., Wang, Q., Dou, X., Wang, W., Zhao, Q., Lv, R., Zhang, H., Zheng, X., Wang, P., Zhang, Z., 2012. MoSwi6, an APSES family transcription factor, interacts with MoMps1 and is required for hyphal and conidial morphogenesis, appressorial function and pathogenicity of *Magnaporthe oryzae*. Mol. Plant Pathol. 13, 677–689.

Rao, P.S., Niederpruem, D.J., 1969. Carbohydrate metabolism during morphogenesis of *Coprinus lagopus* (*sensu* Buller). J. Bacteriol. 100, 1222–1228.

Salame, T.M., Knop, D., Tal, D., Levinson, D., Yarden, O., Hadar, Y., 2012. Predominance of a versatile-peroxidase-encoding gene, *mnp4*, as demonstrated by gene replacement via a gene targeting system for *Pleurotus ostreatus*. Appl. Environ. Microbiol. 78, 5341–5352.

Schiphof, K., Kawauchi, M., Tsuji, K., Yoshimi, A., Tanaka, C., Nakazawa, T., Honda, Y., 2024. Functional analysis of basidiomycete specific chitin synthase genes in the agaricomycete fungus *Pleurotus ostreatus*. Fungal Genet. Biol. 172, 103893.

Szewczyk, E., Nayak, T., Oakley, C.E., Edgerton, H., Xiong, Y., Taheri-Talesh, N., Osmani, S.A., Oakley, B.R., 2006. Fusion PCR and gene targeting in *Aspergillus nidulans*. Nat. Protoc. 1, 3111–3120.

Yano, S., Suyotha, W., Honda, A., Takagi, K., Rattanakit-Chandet, N., Wakayama, M., Tachiki, T., 2011. N-terminal region of chitinase I of *Bacillus circulans* KA-304 contained new chitin-biding domain. Biosci. Biotechnol. Biochem. 75, 299–304.

Zhang, G., Ren, A., Shi, L., Zhu, J., Jiang, A., Shi, D., Zhao, M., 2018. Functional analysis of an APSES transcription factor (*GlSwi6*) involved in fungal growth, fruiting body development and ganoderic-acid biosynthesis in *Ganoderma lucidum*. Microbiol. Res. 207, 280–288.

Zhao, Y., Su, H., Zhou, J., Feng, H., Zhang, K.Q., Yang, J., 2015. The APSES family proteins in fungi: characterizations, evolution and functions. Fungal Genet. Biol. 81, 271–280.